Analytical Modeling of Switched Flux Memory Machine

Hui Yang, Heyun Lin, *Senior Member, IEEE*, Yibo Li, Haitao Wang, Shuhua Fang, and Yunkai Huang

Engineering Research Center for Motion Control of Ministry of Education, Southeast University, Nanjing 210096, China

This paper presents simple analytical modelling for switched flux memory machine to provide in-depth insight into the operating mechanism. The analytical approach is based on the slotless open-circuit air-gap flux density and the slotted air-gap relative permeance calculations for a doubly salient structure. This allows rapid calculation of several electromagnetic characteristics, e.g. air-gap flux density, flux linkage, back electromotive force (EMF), average torque, etc. Thus, the relationship between various design parameters can be identified, which aids the establishment of the design guideline for this type of machine. The analytical and FE models have been validated by experiments.

***Index Terms*—Analytical modeling, finite element, memory machine, permanent magnet, switched flux, variable flux.**

I. Introduction

DUE TO high efficiency and torque density, rare-earth permanent magnet (PM) machines have been commercialized in many industrial applications [1]. Nevertheless, conventional PM machines generally suffer from limited flux-weakening capability and constant power operating region, which are undesired for wide-speed-range applications. Therefore, variable-flux PM (VFPM) machines [1] were extensively regarded as a viable solution to allow PM machines to offer an extended speed range with high efficiency in the high speed region.

As a newly emerged VFPM machine, memory machine was proposed by V. Ostovic [2]. Recently, the concept of the "memory machine" extended to stator excited machines [3]-[5] having both PMs and DC coils on the stationary side, i.e., DC-magnetized memory machines. The current pulses are energized by the DC magnetizing coils, which facilitates the online magnetization control. Doubly salient (DS) structures [3]-[4] consisting of two stator layers were proposed, which have the advantages of good rotor robustness and easy thermal dissipation. However, they suffer from high torque ripple. Then, the switched flux topologies [5] were applied to memory machines, i.e. so-called switched flux memory machines (SFMMs). The SFMMs realize energy-efficient flux regulation due to the utilization of low coercive force (LCF) PMs. Moreover, the bipolar and sinusoidal flux-linkage allow standard three-phase inverters available for drives. Thus, the torque capability of SFMMs can be improved relative to the DS topologies.

Nevertheless, the existing literature is restricted to FE-based analysis and performance evaluation in individual cases, and no general analytical modeling for SFMM has been reported to provide in-depth understanding of the operating mechanism of SFMMs. Indeed, the electromagnetic design of SFMMs is quite different from those conventional PM machines due to their exclusive features such as performance requirement on different magnetization levels. Hence, the design effort appear to be sophiscated due to various conflict between electromagnetic parameters. Thus, a computationally efficient design method is required to simplify design effort.

To fill this gap, a simple analytical modeling based on the slotless open-circuit air-gap flux density [7] and the slotted air-gap relative permeance calculations [8] is presented to facilitate the preliminary design effort. It should be noted that this analytical model is applicable for those hybrid magnet SFMM as well. The design considerations for magnet sizing is introduced based on the analytical modeling and a developed virtual linear hysteresis model. Besides, the stator/rotor pole combination is optimized with the aid of analytical modeling. Then, the several electromagnetic characteristics, e.g. air-gap flux density, flux linkage, back electromotive force (EMF), average torque will be predicted analytically and compared with finite element method (FEM) results. Finally, the analytical and FEM predictions are validated by measurements.

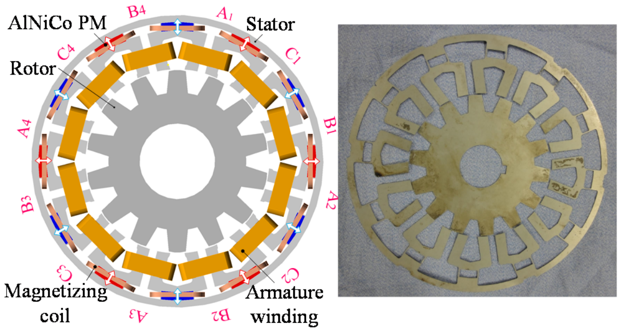

(a) (b)
Fig. 1. Topology of SFMM. (a) Configuration. (b) Cross-sectional view.

II. Analytical Model of SFMM

A. Machine Configuration

Fig. 1 illustrates the proposed machine topology and prototyped lamination, which features a doubly salient structure. In the stator, the diametrically magnetized AlNiCo PMs with alternative polarities are embedded between the "U"-shape stator-tooth modules and stator yokes, the magnetizing coils are accommodated in the outer side slots adjacent to the PMs. The salient-pole rotor can be simply made of laminated silicon steel sheets without any magnets and coils, which is highly mechanically robust. As transient current pulses are applied in the magnetizing coils, the PMs adjacent to the coils can be either magnetized or demagnetized, thereby achieving the flux-regulation. The experimental results will be given in the full paper.

B. Analytical Model

Fig. 2 shows the simplified analytical model of SFMM. Due to the doubly salient structure, the analytical model can be categorized into three layers, namely, 1) AlNiCo PM excitation, which is similar to conventional surface-mounted PM configuration; 2) salient stator module, which consists of several "U"-shape segments; 3) salient rotor teeth, which resemble the conventional switched reluctance machine. Hence, the open-circuit air-gap flux density can be rapidly obtained by multiplying stationary PM MMF and air-gap permeance formed by stator/rotor doubly saliency.

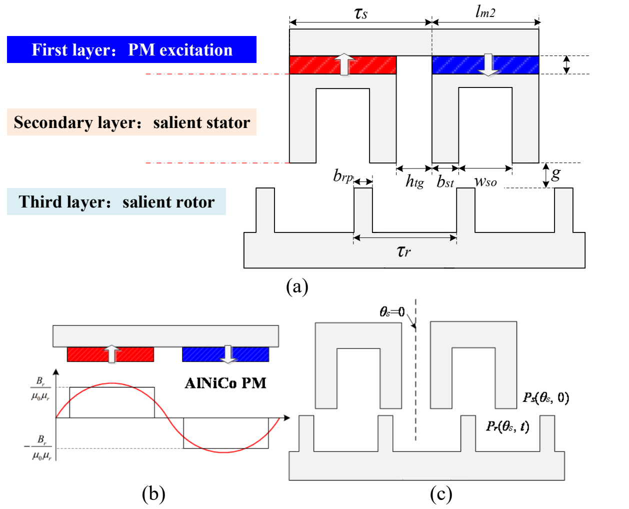

Fig. 2. Analytical model of SFMM. (a) Simplified model. (b) PM MMF. (c) Salient stator and rotor models.

1) PM MMF

According to equivalent analytical model, PM MMF can be formatted as

$$F_m = \sum_{i=1,3,5...}^{\infty} F_i \cos(iN_s\theta_s) = \sum_{i=1,3,5...}^{\infty} \frac{4B_r h_m}{\pi\mu_0\mu_r}\sin\left(\frac{i\alpha_{pm}\pi}{2}\right)\cos(iN_s\theta_s) \quad (1)$$

where F_i is ith harmonic of PM MMF, θ_s is relative position of stator and rotor teeth, B_r is the PM remanence, h_m is PM thickness, α_{pm} is PM pole arc coefficient.

2) Air-Gap Permeance

The air-gap permeance due to slotted stator/rotor doubly saliency can be given by

$$\lambda_s(\theta_s) = \lambda_0 + \lambda_1\cos(2N_s\theta_s) \quad (2)$$

$$\lambda_r(\theta_s,t) = \lambda_0 + \lambda_1\cos(Z_r\theta_s - Z_r\omega_r t) \quad (3)$$

where ω_i is rotor angular speed. λ_0 and λ_1 denote DC and fundamental components, which can be expressed by

$$P_0 = \frac{\mu_0(1-1.6\beta b_0/t)}{(g+h_m/\mu_0)} \quad (4)$$

$$P_1 = \frac{4\mu_0\beta\left[\left(0.5+\frac{(b_0/t)^2}{0.78125-2(b_0/t)^2}\right)\right]}{\pi(g+h_m/\mu_0)}\sin\left(1.6\pi\frac{b_0}{t}\right) \quad (5)$$

$$\beta = 0.5 - \frac{1}{2\sqrt{1+\left(\frac{b_0}{2g+2h_m/\mu_0}\right)^2}} \quad (6)$$

where b_0 is stator slot width. It should be noted that the stator slot opening b_0 equals b_{st} similar to conventional SFPM counterparts.

3) Air-Gap Flux Density

The air-gap flux density can be calculated by multiplying PM MMF and air-gap permeance, i.e.

$$B_g(\theta_s,t) = F_m(\theta_s,t)\times\lambda_{sr}(\theta_s,t) \quad (7)$$

III. PRELIMINARY ANALYSIS RESULTS

The air-gap flux density waveforms and harmonic spectra predicted by analytical method and FEA are plotted in Fig. 3. Basically, the analytically and FE predicted results agree. Specifically, the analytically calculated magnitudes of the major air-gap flux harmonics are slightly higher than those FE results, which is mainly attributed to the fact that the localized magnetic saturation and flux leakage in the analytical method. In addition, since the localized results predicted by analytical model and FEA in the peak regions show slightly higher discrepancy. The analytical modeling will be refined to account for localized flux leakage to improve its accuracy.

It is noteworthy that the detailed optimization results and performance evaluation, and experiments will be given in the full paper.

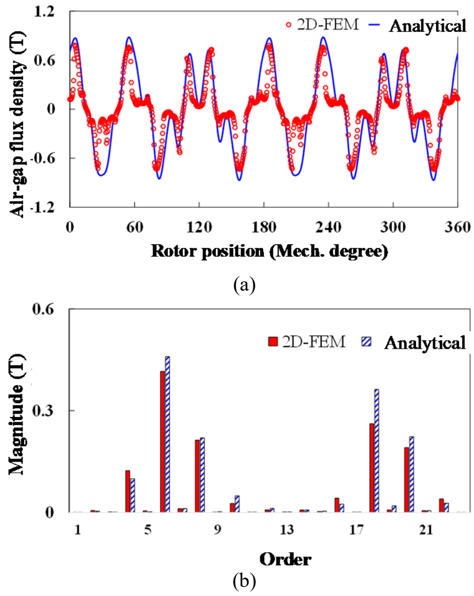

Fig. 3. Comparison of analytically and FE predicted air-gap flux density. (a) Waveform. (b) Harmonic spectra.

REFERENCES

[1] Z. Q. Zhu and D. Howe, "Electrical machines and drives for electric, hybrid, and fuel cell vehicles," *Proc. IEEE*, vol. 95, no. 4, pp. 746-765, Apr.2007.

[2] V. Ostovic, "Memory motors," *IEEE Ind. Appl. Mag.*, vol. 9, no. 1, pp. 52-61, Jan./Feb. 2003.

[3] C. Yu and K. T. Chau, "Design, analysis, and control of DC-excited memory motors," *IEEE Trans. Energy Convers.*, vol. 26, no. 2, pp. 479-489, Jun. 2011.

[4] X. Zhu, L. Quan, D. Chen, M. Cheng, Z. Wang, and W. Li, "Design and analysis of a new flux memory doubly salient motor capable of online flux control," *IEEE Trans. Magn.*, vol. 47, no. 10, pp. 3220-3223, Oct. 2011.

[5] H. Yang, Z. Q. Zhu, H. Lin, S. Fang, and Y. Huang, "Comparative study of novel variable-flux memory machines having stator permanent magnet topologies," *IEEE Trans. Magn.*, vol. 51, no. 11, Article. 8114104, Nov. 2015.

[6] Z. Q. Zhu, D. Howe, and C. C. Chan, "Improved analytical model for predicting the magnetic field distribution in brushless permanent-magnet machines," *IEEE Trans. Magn.*, vol. 38, no. 1, pp. 229–238, Jan. 2002.

[7] D. Zarko, D. Ban, and T. A. Lipo, "Analytical calculation of magnetic field distribution in the slotted air gap of a surface permanent-magnet motor using complex relative air-gap permeance," *IEEE Trans. Magn.*, vol. 42, no. 7, pp. 1828–1837, Jul. 2006.